Article

Using CO₂ as a Cooling Fluid for Power Plants: A Novel Approach for CO₂ Storage and Utilization

Tran X. Phuoc * and Mehrdad Massoudi *

National Energy Technology Laboratory (NETL), U.S. Department of Energy, 626 Cochrans Mill Road,
P.O. Box 10940, Pittsburgh, PA 15236, USA

* Correspondence: Phuoc.Tran@netl.doe.gov (T.X.P.); Mehrdad.Massoudi@netl.doe.gov (M.M.);
Tel.: +1-412-386-6024 (T.X.P.); +1-412-386-4975 (M.M.)

Abstract: To our knowledge, the potential use of CO_2 as a heat-transmitting fluid for cooling applications in power plants has not been explored very extensively. In this paper, we conduct a theoretical analysis to explore the use of CO_2 as the heat transmission fluid. We evaluate and compare the thermophysical properties of both dry air and CO_2 and perform a simple analysis on a steam-condensing device where steam flows through one of the flow paths and the cooling fluid (CO_2 or air) is expanded from a high-pressure container and flows through the other. Sample calculations are carried out for a saturated-vapor steam at 0.008 MPa and 41.5 °C with the mass flow rate of 0.01 kg/s. The pressure of the storage container ranges from 1 to 5 MPa, and its temperature is kept at 35 °C. The pressure of the cooling fluid (CO_2 or dry air) is set at 0.1 MPa. With air as the heat-removing fluid, the steam exits the condensing device as a vapor-liquid steam of 53% to 10% vapor for the container pressure of 1 to 5 MPa. With CO_2 as the heat-removing fluid, the steam exits the device still containing 44% and 7% vapor for the container pressure of 1 MPa and 2 MPa, respectively. For the container pressure of 3 MPa and higher, the steam exits the device as a single-phase saturated liquid. Thus, due to its excellent Joule–Thomson cooling effect and heat capacity, CO_2 is a better fluid for power plant cooling applications. The condensing surface area is also estimated, and the results show that when CO_2 is used, the condensing surface is 50% to 60% less than that when dry air is used. This leads to significant reductions in the condenser size and the capital costs. A rough estimate of the amount of CO_2 that can be stored and utilized is also carried out for a steam power plant which operates with steam with a temperature of 540 °C (813 K) and a pressure of 10 MPa at the turbine inlet and saturated-vapor steam at 0.008 MPa at the turbine outlet. The results indicate that if CO_2 is used as a cooling fluid, CO_2 emitted from a 1000 MW power plant during a period of 250 days could be stored and utilized.

Keywords: heat transfer fluid; Joule–Thomson effect; CO_2 storage; steam condensation; power plant cooling

1. Introduction

In power plants, water is used to remove heat from a wide variety of sources. In cooling application, water is withdrawn from underground, nearby lakes, rivers, and ocean and is diverted and circulated to absorb heat from a wide variety of sources, and then it is discharged back to its original source. Since the discharged water is highly contaminated and its temperature is high, it can cause severe environmental problems. For example, it increases the temperature of our rivers, lakes, and ocean waters, harming marine lives, degrading aquatic ecosystems, etc. For thermal power plants in areas lacking ample water, fresh water must be delivered from far-away places which consumes energy and adds to the cost. Power plants utilizing water for cooling are also vulnerable to power disruptions due to shutdowns or curtailments during times of drought and extreme heat. In addition, water is corrosive, and as it flows, it corrodes the walls of the pipes, the turbine blades, etc.

In addition, in arid regions, water is a sparse and valuable commodity, and water losses during fluid circulation can present a significant economic liability and burden on the ecosystem. A few recent studies point to the use and storage of CO_2 in various applications (see [1–3]).

Air cooling (throughout this paper we use the term 'air' for 'dry air') of thermal power plants has been used in a few isolated instances [4–7]. With air cooling, the exhaust vapor-liquid steam from the turbine generator is circulated through a series of finned tubes in a condenser and is cooled down by a stream of ambient air blown by fans over the tubes. Although air is environmentally preferred and a useful alternative for power plant cooling where water is not available, due to its low overall heat transfer rate per unit surface area, air cooling has many disadvantages. The low overall heat transfer rate per unit surface area requires an increase in steam condensation temperature and associated saturation pressure. This leads to higher steam turbine back pressure which decreases the turbine output and reduces the overall plant efficiency. The low overall heat transfer rate per unit surface area requires relatively larger modules with significant heat transfer enhancements to achieve similar performance levels to water cooling systems, even at higher initial temperature differences. This leads to higher energy costs for cooling fans and higher capital costs. The effectiveness of air cooling depends on the ambient air temperature and humidity. At higher ambient air temperatures, there is a decrease in the rate of thermal energy from the steam to the air. Thus, power plants in hot and arid areas require higher fan work and have lower plant efficiency.

Many studies in geothermal heat mining (see [8–17]) have reported that CO_2 is a better geothermal heat extraction fluid than water. Following these studies, in this paper, we evaluate and compare the thermophysical properties of both CO_2 and air to explore the use of CO_2 as the cooling fluid for thermal power plant applications. The critical temperature and pressure of CO_2 are 31.04 °C and 7.382 MPa, and thus a low temperature flow of supercritical CO_2 can be created. Flow rates for a given driving force are proportional to the ratio of the density of the fluid to its viscosity, $\dot{m} \propto \rho/\mu$. The sensible heat carried by mass flow is proportional to the specific heat of the fluid. The density of supercritical CO_2 is $\rho = 636$ kg/m^3, and its viscosity is $\mu = 50.623$ μPa-s and $c_p = 1.08$ kJ/kg-K, while for water, these values are 998.80 kg/m^3 and 1084.0 μPa-s, 4.18 kJ/kg, and for air, at 0.1 MPa, the density is 1.16 kg/m^3, viscosity is 18.55 μPa-s, and $c_p = 1.06$ kJ/kg-K. The sensible heat carried by CO_2 is about 4 times more than that by water and 215 times more than air. At lower (subcritical) temperatures and/or pressures, CO_2 can be used in two different ways, a liquid, or a gaseous state, as well as two-phase mixtures of these states. An additional important parameter is the Joule–Thomson coefficient (see [18,19]). The Joule–Thomson effect describes the change in temperature of a real gas or liquid when it flows through a valve or porous plug without heat and work interactions with the environment. For CO_2, the Joule–Thomson coefficient can be up to 10 times higher than that of air for the range of pressures up to 5 MPa at temperatures of about 40 °C. Thus, a flow of CO_2 at much lower temperature can be generated to remove more heat as compared to that from an air stream. To obtain a rough estimate for the amount of CO_2 that can be stored and utilized, we hypothetically consider a steam power plant where the steam at 540 C (813 K) and 10 MPa expands through a turbine to become a saturated-vapor steam at 0.008 MPa (saturated temperature is 41.5 C (314.5 K)). The conditions used here might be found in a typical power plant, but it is not for any specific power plant. To increase the overall plant efficiency, exhaust steam needs to be condensed in low-pressure tubes (about 10 to 20 kPa). If supercritical CO_2 is used, the tubes carrying low-pressure steam have to be exposed to a high-pressure environment (>7.3 MPa). Thus, using supercritical CO_2 to remove the condensation heat might not be suitable. There are very few studies related to the power plant cooling using CO_2 as the cooling fluid; in this paper, we propose that CO_2, from various sources, is first captured where excess solar (or wind) energy is used to compress the captured CO_2. This is then stored in a high-pressure container. When it is needed, the compressed CO_2 can be expanded at constant enthalpy into multiple

lower-pressure (0.1 MPa) flow paths that circulate, removing the excess heat from the various components of a thermal power plant. The flow paths and the high-pressure container are designed in a closed-loop arrangement so that the exhaust low-pressure CO_2 streams cannot escape but are collected and compressed again. Thus, using CO_2 for cooling purposes in power plants can offer a novel approach for CO_2 storage and utilization. Since we need to explore the possibility of using CO_2 instead of air, in the following sections, we discuss the thermophysical properties of dry air and CO_2 under subcritical states.

2. Thermodynamic and Transport Properties

In this work, the correlations reported by Span and Wagner [20] for calculating CO_2 density and the correlations developed by Vesovic et al. [21] and Fenghour et al. [22] for the transport properties of CO_2 are used. Using these correlations, we calculate the thermodynamic and transport properties of CO_2 for temperatures ranging from 300 K to 600 K and for pressures up to 60 MPa; we then compare the results with those obtained from the NIST database [23]. The average deviations of about 0.2% to 2.5% are obtained for the thermal conductivity and less than 0.1% for all other properties. For air, we found that the correlation reported by Kadoya [24] is valid for temperatures higher than 1273 K while the equation of state reported by Lemmon et al. [25,26] is applicable for the temperatures ranging from 59.75 K to 2000 K and for pressures up to 2000 MPa. In the range from the solidification point to 873 K at pressures of 70 MPa, the uncertainty of the density values calculated using the equation of state reported in [25,26] is 0.1%. For the transport properties, the correlations reported in [24] can predict both thermal conductivity and viscosity with less than 0.3% uncertainty for the range of temperatures from 300 K to 600 K and pressures up to 100 MPa. Thus, we decided to use these equations in our present study.

Figure 1 shows the thermal and transport properties of both gaseous CO_2 and air in the range of pressures and temperatures that are typically found in practical power plant cooling applications. Effects of both pressure and temperature on these properties are shown. The thermal conductivities of both gaseous CO_2 and air increase slightly with temperature but significantly when pressure increases. By comparing the thermal conductivity and the viscosity of the gaseous CO_2 and air for the range of pressures and temperatures reported here, it can be seen that the air viscosity is about 1.2 times higher than that of CO_2 and the thermal conductivity of air is about 1.3 times higher than that of CO_2. The specific heat of CO_2 is somewhat lower than that of air. The density of CO_2 is about 1.5 times higher than that of air.

Although air has higher specific heat and thermal conductivity than those of CO_2, the flow heat capacity of CO_2, which is proportional to $\rho c_p / \mu$, is found to be more than 1.6 times higher than that of air for the range of pressures and temperature used here (see Figure 2). Thus, it means that, for the same driving force, the ability of CO_2 to remove heat is significantly higher than that of air.

In addition to the flow heat capacity, the cooling effectiveness of a fluid also depends on its initial temperature when it enters a cooling device. This temperature can be controlled by an important property called the Joule–Thomson coefficient. The coefficient describing such effect, μ_{JT}, which depends on the type of gas and on the temperature and pressure of the gas before expansion, is given as (see [27], p. 250))

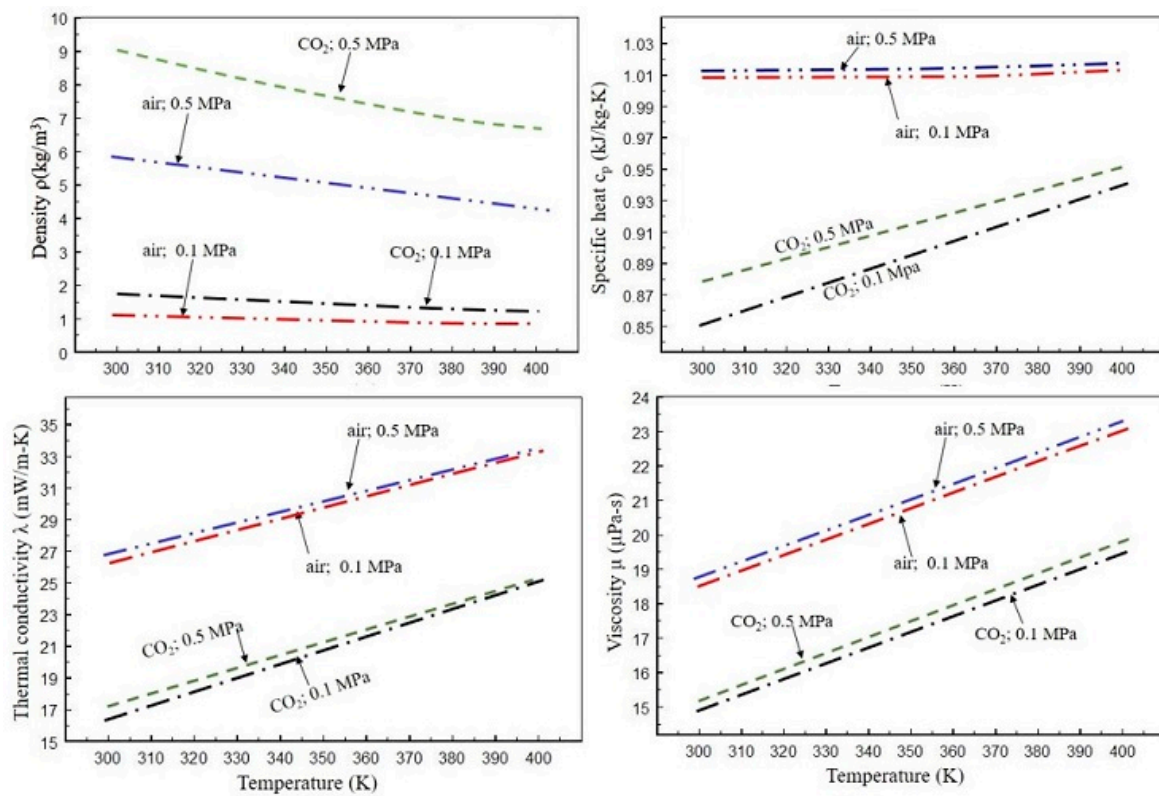$$\mu_{JT} = \left(\frac{\partial T}{\partial P} \right)_h \tag{1}$$

Figure 1. Thermophysical properties of gaseous CO_2 and air for pressures from 0.1 to 0.5 MPa and temperature from 300 to 400 K.
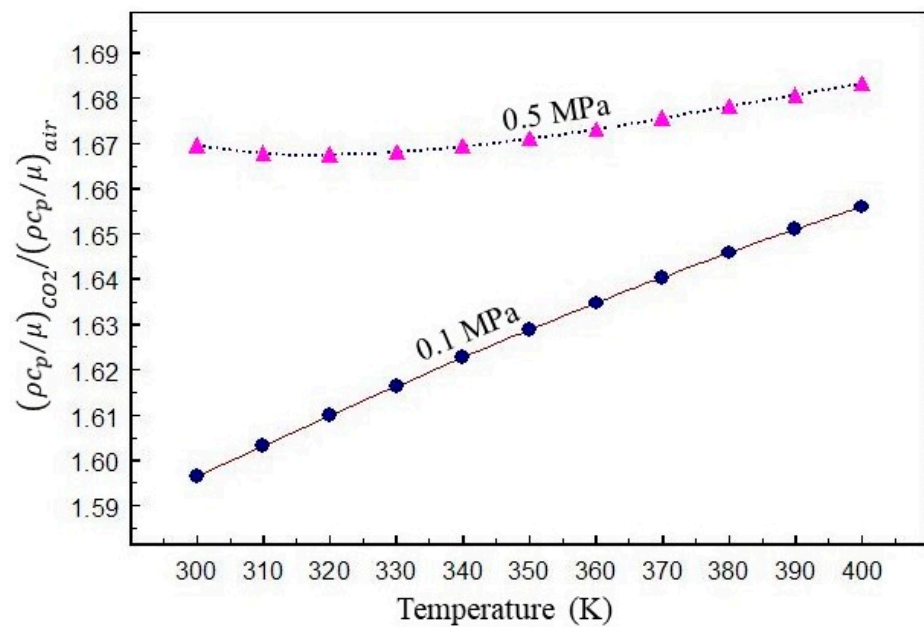

Figure 2. Flow heat capacity of gaseous CO_2 and air.

From Equation (1), the temperature and the mass flux $\dot{m}''_{fl}$ (kg/m²-s) of a fluid in a flow path after it expands from a high-pressure container is approximated as

$$T_{fl} \approx T_{stor} - \mu_{JT}\left(P_{stor} - P_{fl}\right) \tag{2}$$

$$\dot{m}''_{fl} = \rho_{fl} \left(\frac{P_{stor} - P_{fl}}{\rho_{fl}} \right)^{1/2} \tag{3}$$

where P_{stor} is the pressure of the fluid in the high-pressure container, and P_{fl}, ρ_{fl} are the pressure and density of the fluid in the flow path, respectively. Thus, the initial temperature of the fluid entering a cooling device depends on the Joule–Thomson coefficient, the pressure and temperature in the high-pressure container, and the pressure of the flow path. It is clear that when a fluid expands from a high-pressure reservoir into a lower-pressure flow network, since $\partial P < 0$, it is cooled down if μ_{JT} is positive and it is heated if μ_{JT} is negative.

The coefficient μ_{JT} depends on the type of gas being used and, on the temperature, and pressure of the gas before the expansion. The point at which the coefficient μ_{JT} changes its sign is called the inversion point, and the temperature of this point also depends on the pressure of the gas before expansion. From the correlations reported by Span and Wagner [20] for CO_2 and the correlations reported by Kadoya et al., [24] and by Lemmon et al., [25,26] for air, we calculate the Joule–Thomson temperature inversion curves for CO_2 and air (the temperature inversion curve is the curve that connects the inversion point at which the value of the Joule–Thomson coefficient changes sign). The results are shown in Figure 3. The curve divides the graph into two regions: the cooling and the heating regions. If the pressure and temperature before the expansion of a fluid fall into the cooling region, the fluid will be cooled down if it expands at constant enthalpy, and if they fall into the heating region, heating of the fluid ensues.
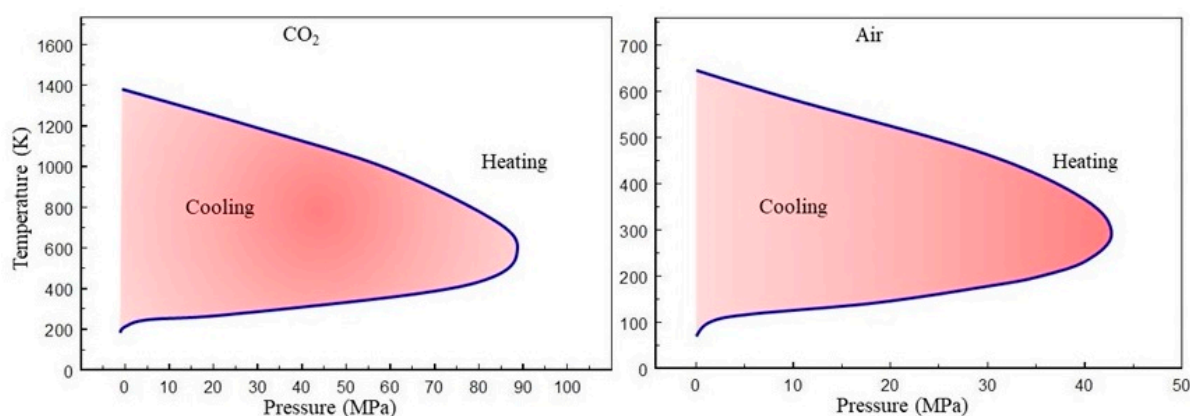

Figure 3. The Joule–Thomson temperature inversion curve for CO_2 and air.

The cooling region for air covers a range of temperature from about 100 K to 650 K and a pressure range up to 42.5 MPa. The cooling region associated with CO_2 has a much bigger range in both pressure and temperature. Let us assume that both gaseous CO_2 and air are stored in a container with pressures ranging from 1 to 5 MPa and are in thermal equilibrium with the surroundings so that the temperature of the stored gas can be somewhere from 35 °C (308 K) to 40 °C (313 K). These conditions fall into the cooling regions of both CO_2 and air as shown in Figure 3. Thus, as these gases expand, the temperature of the expanded streams entering a cooling device will be lower than their temperatures in the storage container. However, the values of μ_{JT} of CO_2 are 4.9 to 5.6 times higher than those of air as shown in Figure 4, and the temperature of the CO_2 entering a cooling device, as given by Equation (2), depends on the storage tank temperature and the pressure, and it is 7 to 40 K lower than that of air. The data are based on the correlations reported by Span and Wagner [20] for CO_2 and the correlations reported by Kadoya et al. [24] and by Lemmon et al. [25,26] for air.
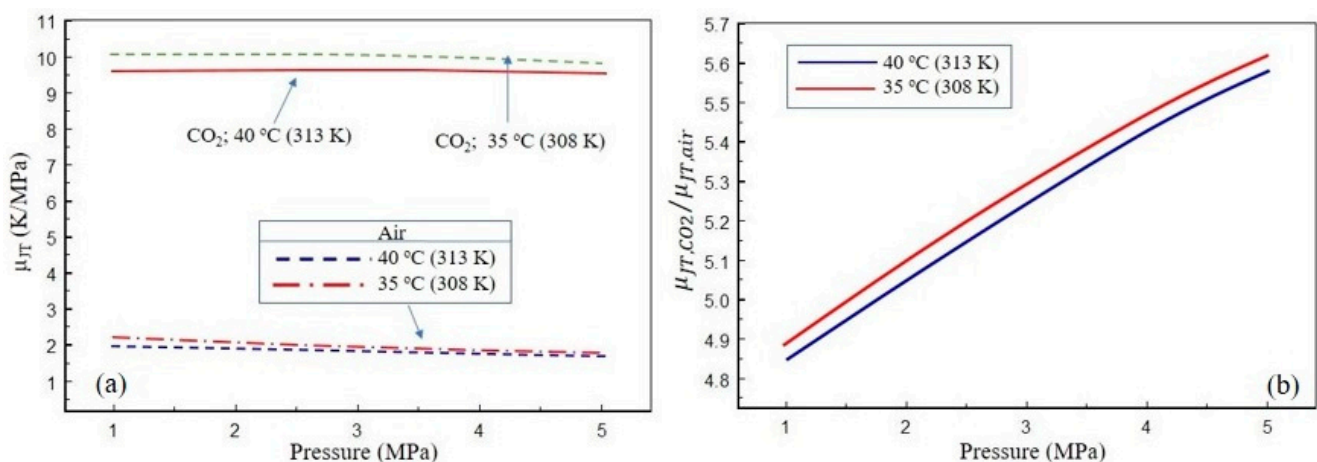
Figure 4. The Joule–Thomson coefficient of gaseous CO_2 and air as a function of the temperature and pressure before expansion, ((**a**): Joule-Thomson coefficient of CO_2 and air; (**b**): Ratio of the CO_2 Joule-Thomson coefficient to the air Joule-Thomson coefficient).

As an example, we use Equation (2) to calculate the fluid temperature entering a cooling device which is operated at a constant pressure of 0.1 MPa after the expansion from a high-pressure container. The container pressures are from 1 to 5 MPa, and the surrounding temperatures are at 35 °C (308 K) and 40 °C (313 K). The results are tabulated in Table 1. For the same conditions, the temperature of the CO_2 stream is significantly lower than that of air while the mass flux of the CO_2 stream is significantly larger than that of air. These results indicate that using CO_2 for cooling is much more effective than using air.

Table 1. Temperature and mass flux, $\dot{m}''$ (kg/m^2-s), of CO_2 and air entering a cooling device at MPa after being expanded from a high-pressure container.

Container		T_{in} and Mass Flux, $\dot{m}''$ (kg/m^2-s), Entering a Cooling Device			
P	T	T_{in}		$\dot{m}''$	
(MPa)	(K)	(K)		(kg/m^2-s)	
		CO_2	Air	CO_2	Air
1.0	308	299	306	1265	1012
	313	304	311	1253	1003
2.0	308	288	304	1871	1475
	313	294	309	1852	1462
3.0	308	278	302	2354	1827
	313	284	307	2327	1812
4.0	308	268	300	2781	2125
	313	275	306	2746	2106
5.0	308	259	299	3176	2388
	313	266	304	3132	2367

3. Steam Condensing Performance

The condenser is an important component of a thermal power plant; it receives and turns the exhausted steam from a turbine into water by basically cooling it. The main function of a condenser is to maintain a low back pressure on the exhaust side of the turbine allowing the turbine to do more work and to convert the discharge steam back to saturated-liquid water before it is pumped back to the steam generator. To accomplish these functions, the condenser must have a high cooling rate to fully remove the heat released due to condensation. In this section, we perform a simple calculation to see if the gaseous CO_2 or air is a better fluid for removing the heat released from steam condensation.

A comprehensive analysis of a steam condenser is not be presented here. Here, we simply consider the problem involving the flow of the steam and of the cooling fluid in a two-flow-path condensation device. A vapor-saturated steam at 0.08 MPa and 41.5 °C is flowing in one flow path. In the other flow path, a cooler fluid (CO_2 or air) is flowing. Such a flow configuration is shown in Figure 5 as an example. For the steam, the temperature and the pressure are assumed to be constant. The pressure of the cold-flow path is also constant, but its temperature increases as it flows through the cold-flow path by absorbing the condensation heat released from the steam-flow path. As the steam flows through its flow path, condensation occurs and liquid water is produced; thus, the flow of steam is a two-phase vapor-liquid flow, where we assume that the velocity of the steam is constant. As the steam is condensed, the condenser pressure might decrease leading to an increase in the velocity as well as a decrease in the saturated temperature; these assumptions can be justified due to the fact that when the steam exits the turbine, it is distributed over a large area of short tubes (more than 20,000 tubes), and any effects due to steam condensation might not be significant. In addition, the main objective of the present work is to compare the effectiveness of dry air and CO_2 when they are used as cooling fluids, and since these assumptions are applied to both air and CO_2, they do not significantly alter the results of the present work. With these assumptions, the following equations are used (see [28]):
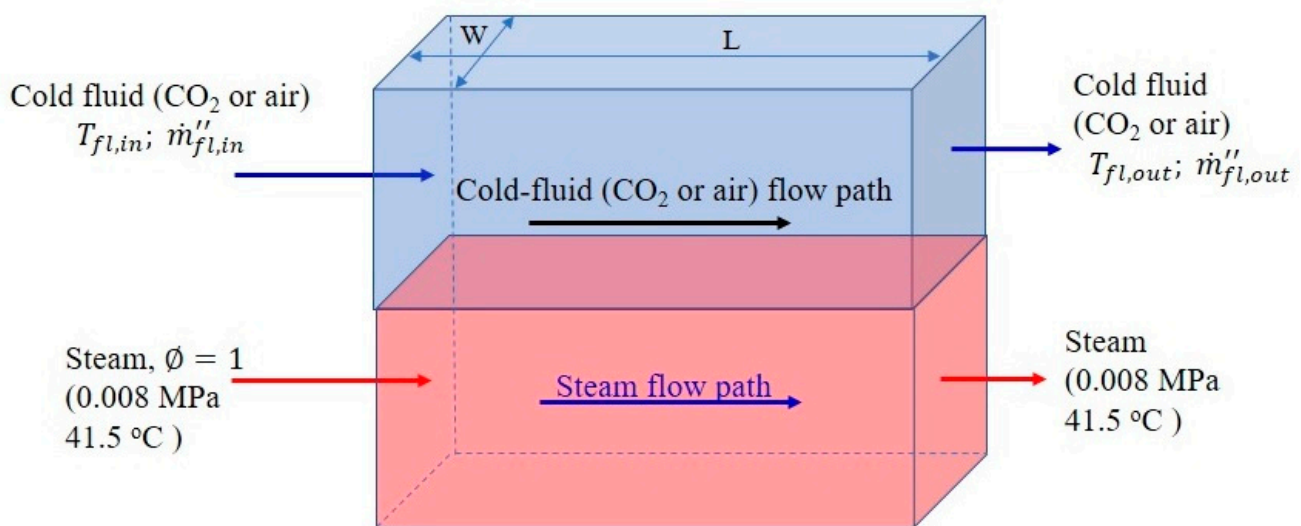

Figure 5. Representation of a steam-condensing device.

3.1. Mass Conservation Equation for the Condensing Steam

$$\frac{d}{dx}[(1-\phi)\rho_w v_x + \phi\rho_v v_x] = 0 \tag{4}$$

where ϕ is the volume fraction of the vapor, ρ_w is the density of the liquid water, ρ_v is the density of the water vapor, and x is the direction of the flow.

3.2. Vapor Conservation Equation

$$\frac{d(\phi\rho_v v_x)}{dx} = -\dot{m}_v''' \tag{5}$$

where v_x is the steam velocity which is assumed to be constant, and $\dot{m}_v'''$ (kg/m³-s) is the steam condensation rate per unit volume. From these equations, the variation of the vapor volume fraction as the steam flows in its path is given by

$$\frac{d\phi}{dx} = -\frac{\dot{m}_v'''}{\rho_w v_x} \tag{6}$$

3.3. Energy Conservation Equation for the Cooling Stream

To keep the steam temperature constant, we assume that the condensation heat released by the steam is fully absorbed by the cooling fluid. Assuming that the temperature of the cold flow is uniform across the flow path, the wall separating the steam and the cold-flow paths has a large thermal conductivity, and the energy equation for the cold flow is

$$\frac{dT_{fl}}{dx} = \frac{Ph_{c,fl}\left(T_{st} - T_{fl}\right)}{\dot{m}_{fl}c_{p,fl}}$$

(7)

where p is the perimeter of the cooling-fluid flow path, and $\dot{m}_{fl}$ (kg/s) and $c_{p,fl}$ are the mass flow rate and the specific heat of the cold fluid, respectively, which are assumed to be constants. To keep the stream temperature and pressure constant, the condensation heat released must be fully removed by the cold fluid, thus, the heat-transfer-controlled condensation rate is calculated as

$$\dot{m}_v''' = \frac{Ph_{c,fl}\left(T_{st} - T_{fl}\right)}{A_{st}h_{fg}}$$

(8)

where h_{fg} is the latent heat of condensation, A_{st} is the cross-sectional area of the steam path, $h_{c,fl}$ is the convective heat transfer coefficient which is related to the Nusselt number, Nu, λ_{fl} is the fluid thermal conductivity, and D is the characteristic length of the cold-fluid stream. Thus,

$$h_{c,fl} = \frac{Nu\lambda_{fl}}{D}$$

(9)

From these equations, we can obtain the fluid temperature and the vapor volume fraction along the flow direction as

$$T_{fl} = T_{st} - \left(T_{st} - T_{fl,in}\right)e^{-\frac{PNu\lambda_{fl}L}{D\dot{m}_{fl}c_{p,fl}}\xi}$$

(10)

$$\phi = \phi_{in} + \left(\frac{\dot{m}_{fl}c_{p,fl}}{A_{st}h_{fg}\rho_w v_x}\right)\left(T_{st} - T_{fl,in}\right)\left(e^{-\frac{PNu\lambda_{fl}L}{D\dot{m}_{fl}c_{p,fl}}\xi} - 1\right)$$

(11)

where $\xi = x/L$, ϕ_{in} is the volume fraction of the vapor of the steam entering the device, T_{st} is the steam temperature, $T_{fl,in}$ is the temperature of the cold steam at the device inlet, and L is the device length. The steam-flow path cross-sectional area, A_{st}, and the velocity v_x in Equation (11) are related via the steam mass flow rate

$$A_{st}v_x = \frac{\dot{m}_{st}}{[\phi_{in}\rho_v + (1 - \phi_{in})\rho_w]}$$

(12)

From Equations (10) and (11), both ϕ and the fluid temperature depend on the flow heat capacity of the cold fluid, $\dot{m}_{fl}c_{p,fl}$, the fluid temperature at the cooling device inlet, $T_{fl,in}$, the exponential power, $\left(\lambda_{fl}\right)/\left(\dot{m}_{fl}c_{p,fl}\right)$, and the heat transfer characteristic of the condensing device, $PNuL/D$, which depends on the condensing device dimension and the Nusselt number. For the condensation to be effective, the value of $PNuL/D$ should be very large since the surface area for heat transfer between the steam and the cold fluid must be very large. For example, to evaluate the thermal performance of a steam surface condenser for a typical 210 MW coal-fired power plant using water as the cooling fluid, Pattanayaka et al., [29] used a condenser equipped with 15,620 tubes having a total surface area of 14,600 m^2.

Example calculations use the following conditions: $PNuL/D = 1.0 \times 10^6$. For the saturated vapor at 0.008 MPa and 41.5 °C: $\rho_v = 0.05524$ kg/m^3, $\rho_w = 0.9917$ kg/m^3, $\phi_{in} = 1$. For the cold fluid, the cross-sectional area $A_{fl} = 0.1$ m^2, and the inlet temperatures are

tabulated in Table 1. The heat capacity of the cold fluid, $\dot{m}_{fl}c_{p,fl}$, and the exponential power, $\left(\lambda_{fl}\right)/\left(\dot{m}_{fl}c_{p,fl}\right)$, are tabulated in Table 2 for easy comparison. The storage pressures are from 1 MPa to 5 MPa and its temperature is kept at 35 °C (308 K). As shown in Table 1, the entering temperatures of CO_2 are about 6 to 7 degrees lower than those of air for the same range of container pressures. Thus, CO_2 is a better heat-removing fluid than air as shown in Figures 6 and 7. Figure 6 shows the effect of the storage pressure on the steam vapor volume fraction. Using air as the heat-removing fluid, the steam exits the cooling device as a two-phase vapor-liquid steam. It has 53% vapor when the container pressure is 1 MPa and 10% vapor when the container pressure is 5 MPa. The results for CO_2 show a significant improvement. At 1 MPa, the steam contains about 44% of vapor when it exits the condensing device, and it contains a negligible vapor amount of 7% when the storage pressure is 2 MPa. When the container pressure is at 3 MPa and higher, the steam becomes a saturated-liquid water before escaping the condensing device. For example, when the steam is cooled by CO_2 which is expanded from the container with pressures of 3, 4, and 5 MPa, the steam becomes a saturated liquid at $\xi = 0.8$, $\xi = 0.66$, and $\xi = 0.58$, respectively. In thermal power plants, the condenser is a very important component. Its function is to produce a saturated liquid water before it is pumped back into the boiler. It also maintains the back pressure on the exhaust side of the turbine. This improves the efficiency of the plant. The results shown here indicate that to meet these functions, CO_2 is a better heat-removing fluid than air for the condenser.
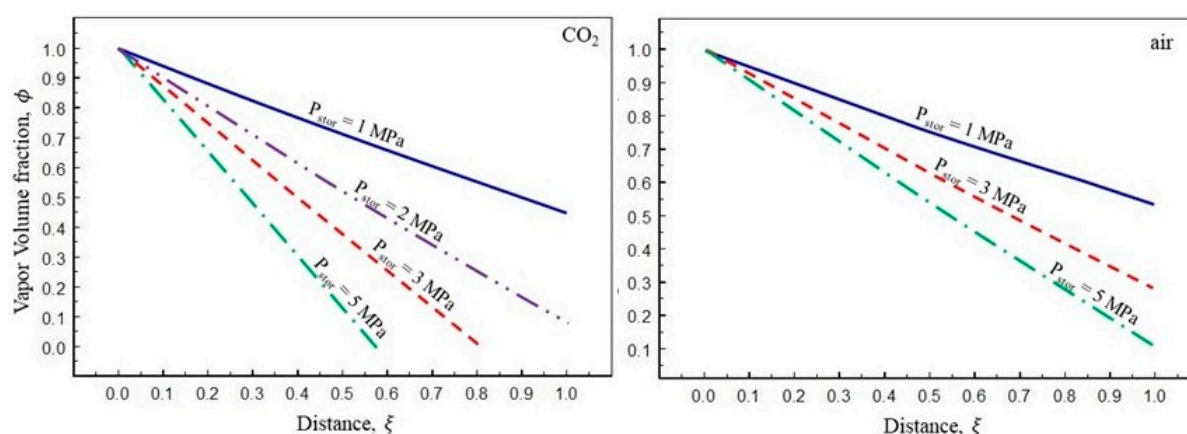

Figure 6. Effect of storage pressure on the volume fraction of the steam vapor (storage container temperature of 35 °C (308 K)).
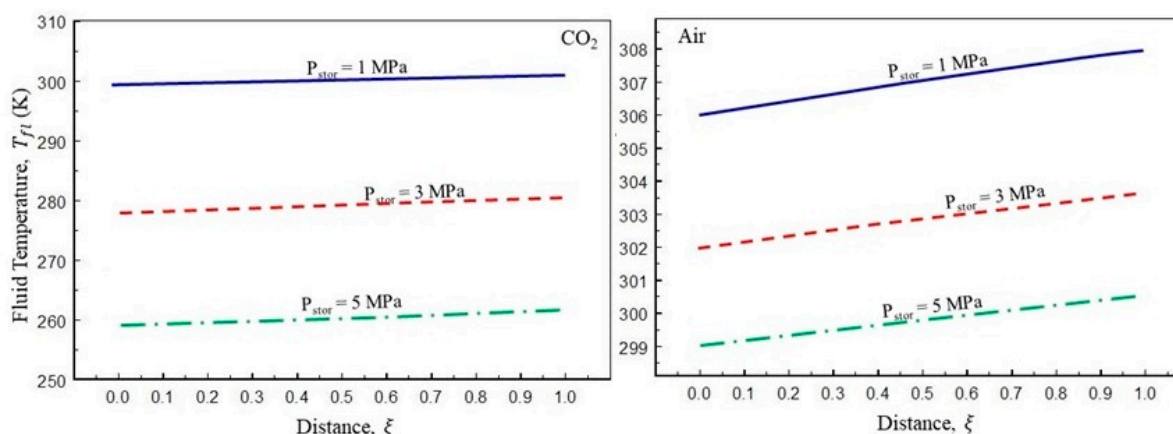

Figure 7. Effect of storage pressure on the cooling-fluid temperature (storage container temperature of 35 °C (308 K)).

Table 2. Heat capacity and exponential power of CO_2 and air for Equations (10) and (11) (cooling device at 0.1 MPa).

Pstor	(MPa)		$\dot{m}_{fl}c_{p,fl}$ (J/s-K)	$(\lambda_{fl})/(\dot{m}_{fl}c_{p,fl})$ (1/m)	
	Air	CO_2	Air	CO_2	
1	101,884	107,702	2.635×10^{-7}	1.55×10^{-7}	
2	148,485	157,302	1.797×10^{-7}	1.00×10^{-7}	
3	183,906	195,623	1.443×10^{-7}	7.68×10^{-8}	
4	213,887	228,415	1.234×10^{-7}	6.24×10^{-8}	
5	240,350	258,122	1.095×10^{-7}	5.26×10^{-8}	

Another benefit of using CO_2, based on this example, is related to the condenser surface area. The results show that when air from the container of pressure of 1 MPa is used as the cooling fluid, the steam exits the condensing device ($\xi = 1$) with 53% vapor and 47% liquid water. This means that as the steam flows through the condensing device, 47% of the vapor content has been condensed. When the pressure of the high-pressure container is 2 MPa, the same amount of vapor can be condensed within a shorter length, $\xi = 0.77$. From Figure 5, if W is the width, the condensing surface area can be roughly calculated as $WL\xi$ which is equal to WL when the container pressure is 1 MPa, and it reduces to 0.77 WL when the container pressure is 2 MPa. We define ξ (47%) to be the length of the condenser where 47% of the vapor content has been condensed. We report in Table 3 the values of ξ (47%) and the corresponding condensing surface areas for the various conditions used here. Depending on the container pressure, the condensing surface area with CO_2 as the cooling fluid could be as low as 50% of the condensing surface area when air is used. This leads to a significant reduction in the condenser size and capital costs.

Table 3. Condenser length, $\xi_{47\%}$, and condenser area, $WL\xi_{47\%}$, required for 47% of vapor content to be condensed.

Pstor	$\xi_{47\%}$		Condenser Area ($WL\xi_{47\%}$)	
(MPa)	Air	CO_2	Air	CO_2
1	1	0.82	WL	0.82 WL
2	0.77	0.49	0.77 WL	0.49 WL
3	0.63	0.37	0.63 WL	0.37 WL
4	0.54	0.30	0.54 WL	0.30 WL
5	0.51	0.27	0.51 WL	0.27 WL

4. CO_2 Storage and Utilization

To obtain a rough estimate for the amount of CO_2 that can be stored and utilized, we hypothetically consider a steam power plant where the steam at 540 °C (813 K) and 10 MPa expands through a turbine to become a saturated-vapor steam at 0.008 MPa (saturated temperature is 41.5 °C (314.5 K)). The steam discharged from the turbine enters a condenser and is condensed to a saturated liquid by a stream of CO_2 as the heat-removing fluid. Neglecting the turbine efficiency, the steam mass flow rate, $\dot{m}_{st}$, is theoretically calculated from the steam work, $\dot{W}_t$, as

$$\dot{m}_{st} = \frac{\dot{W}_t}{(h_{st,in} - h_{st,out})} \tag{13}$$

where $h_{st,in}$ and $h_{st,out}$ are the specific enthalpy of the steam at the turbine inlet and exit, respectively. The equation for the energy rate with isothermal heat released during the steam condensation is given as

$$\dot{Q}_{st} = \dot{m}_{st}h_{fg} = \frac{\dot{W}_t h_{fg}}{(h_{st,in} - h_{st,out})} \tag{14}$$

where h_{fg} is the latent heat of condensation of the steam. The heat absorbed by the cold steam of CO_2 is

$$\dot{Q}_{CO2} = \dot{m}_{CO2}c_{p,CO2}(T_{CO2,in} - T_{CO2,out}) \tag{15}$$

where $\dot{m}_{CO2}$ is the mass flow rate for CO_2, $c_{p,CO2}$ is the CO_2 specific heat, and $T_{CO2,in}$ and $T_{CO2,out}$ are the CO_2 temperatures at the condenser inlet and outlet, respectively. It is required that the energy released during the condensation must be absorbed by the CO_2; the CO_2 mass flow rate is calculated as

$$\dot{m}_{CO2} = \frac{\dot{W}_t h_{fg}}{c_{p,CO2}(h_{st,in} - h_{st,out})(T_{CO2,in} - T_{CO2,out})} \tag{16}$$

As an example, we use the condition of the steam given above ($h_{st,in}$ = 3475.5 kJ/kg, $h_{st,out}$ = 2577 kJ/kg, h_{fg} = 2403 kJ/kg). For CO_2 at 0.1 MPa and $T_{CO2,in}$ = 278 K, the specific heat $c_{p,CO2}$ = 0.85 kJ/kg-K, and assuming that $T_{CO2,out}$ is equal to the steam saturated temperature at 0.008 MPa, $T_{CO2,out}$ = 314.5 K. For a power plant of $\dot{W}_t$ = 1000 MW, the mass flow rate of the CO_2 is roughly calculated as 86,203 kg/s (744,7965 tons/day). It is noted that a large coal-fired power plant of 1000 MW generates approximately 30,000 tons of CO_2 per day [9]; thus, the amount of CO_2 emitted from such a large coal-power plant for 250 days can be stored and utilized.

5. Conclusions

To explore the use of CO_2 as a heat-absorbing fluid for power plant cooling applications, thermophysical and transport properties of CO_2 were evaluated and compared with those of air. The following conclusions can be deduced:

- With its high heat capacity and excellent Joule–Thomson cooling effect, CO_2 is a better and more effective fluid for removing heat from a thermal power plant than air.
- The condenser is an important component in power plants. Its primary function is to produce saturated liquid water before pumping it back into the boiler while maintaining the back pressure on the exhaust side of the turbine. Sample calculations carried out for a simple steam-condensing device shown in Figure 5 indicated that CO_2 is a better heat-removing fluid than air for a condenser to meet these functions.
- The condensing surface area was also estimated, and the results show that when CO_2 is used, the condensing surface is 50% to 60% less than the case if air is used. This leads to significant reductions in the condenser size and capital costs.
- We roughly estimated the amount of CO_2 that can be stored and utilized for a steam power plant that operates with steam of 540 °C (813 K) and 10 MPa at the turbine inlet and saturated-vapor steam at 0.008 MPa at the turbine outlet. The results indicate that if CO_2 is used as a cooling fluid, the CO_2 emitted from a 1000 MW power plant during a period of 250 days can be stored and utilized.

Author Contributions: T.X.P. thought of this problem and performed most of the derivations and all the calculations. M.M. helped in the derivation and the formulation of the problem. Both authors contributed to the writing of the paper. All authors have read and agreed to the published version of the manuscript.

Nomenclature

A_{st} (m^2)	Cross-sectional area of the steam path
$c_{p,fl}$ (J/kg-K)	Fluid-specific heat at constant pressure
$c_{p,CO2}$ (J/kg-K)	CO_2-specific heat at constant pressure
D (m)	Heat transfer characteristic length of the cold-fluid stream
h_{fg} (J/kg)	Latent heat of condensation
$h_{c,fl}$ (J/m^2–s-K)	Convective heat transfer coefficient
$h_{st,in}$ (J/kg)	Specific enthalpy of the steam at the turbine inlet
$h_{st,out}$ (J/kg)	Specific enthalpy of the steam at the turbine exit
L (m)	Length
$\dot{m}''_{fl}$ (kg/m^2–s)	Fluid mass flow rate per unit area
$\dot{m}'''_{v}$ (kg/m^3-s)	Condensation rate
$\dot{m}_{st}$ (kg/s)	Steam mass flow rate
$\dot{m}_{CO2}$ (kg/s)	CO_2 mass flow rate
Nu	Nusselt number, N_u
P (m)	Perimeter of the cold-fluid flow path
P_{stor} (Pa)	Storage container pressure
P_{fl} (Pa)	Fluid pressure in the condenser
$\dot{Q}_{st}$ (J/s)	Isothermal heat released rate during steam condensation
$\dot{Q}_{CO2}$ (J/s)	Rate of heat absorbed by CO_2 stream
$T_{CO2,in}$ (K)	CO_2 temperature at the condenser inlet
$T_{CO2,out}$ (K)	CO_2 temperature at the condenser outlet
T_{st} (K)	Steam temperature
$T_{fl,in}$ (K)	Cold-fluid temperature at the condenser inlet
μ_{JT} (K/Pa)	Joule–Thomson coefficient
T_{fl} (K)	Fluid temperature in the condenser
T_{stor} (K)	Fluid temperature in the storage container
ρ_{fl} (kg/m^3)	Fluid density
x (m)	x-direction
v_x (m/s)	Steam velocity in x-direction
$\dot{W}_t$ (J/s)	Turbine work
λ_{fl} (J/m-s-K)	The fluid thermal conductivity
ξ	Dimensionless distance
ρ_w (kg/m^3)	Density of liquid water
ρ_v (kg/m^3)	Density of the vapor
ϕ	Volume fraction of the vapor
ϕ_{in}	Vapor fraction of the steam at the condenser inlet

References

1. Cho, J.; Park, G.; Kwon, S.; Lee, K.S.; Lee, H.S.; Min, B. Compositional Modeling to Analyze the Effect of CH4 on Coupled Carbon Storage and Enhanced Oil Recovery Process. *Appl. Sci.* **2020**, *10*, 4272. [CrossRef]
2. Hou, S.-S.; Chiang, C.-Y.; Lin, T.-H. Oxy-Fuel Combustion Characteristics of Pulverized Coal under O_2/Recirculated Flue Gas Atmospheres. *Appl. Sci.* **2020**, *10*, 1362. [CrossRef]
3. Yokoyama, R.; Ohkura, M.; Nakamata, T.; Wakui, T. Numerical Analysis for Performance Evaluation of a Multi-Functional CO_2 Heat Pump Water Heating System. *Appl. Sci.* **2018**, *8*, 1829. [CrossRef]
4. O'Donovan, A.; Grimes, R. A theoretical and experimental investigation into the thermodynamic performance of a 50 MW power plant with a novel modular air-cooled," Condenser. *Appl. Therm. Eng.* **2014**, *71*, 119–129. [CrossRef]
5. Lin, J.; Mahvi, A.J.; Kunke, T.S.; Garimella, S. Improving air-side heat transfer performance in air-cooled power plant condensers. *Appl. Therm. Eng.* **2020**, *170*, 114913. [CrossRef]

6.   Mahvi, A.J.; Kunke, T.; Crystal, R.V.; Garimella, S. Enhanced Power Plan Air-Cooled Condenser Using Auto-Fluttering Reads. *Appl. Therm. Sci.* **2021**, *193*, 116956. [CrossRef]

7.   Bustamante, J.G.; Rattner, A.S.; Garimella, S. Achieving near-water-cooled power plant performance with air-cooled condensers. *Appl. Therm. Eng.* **2016**, *105*, 362–371. [CrossRef]

8.   Pritchett, J.W. On the relative effectiveness of H_2O and CO_2 as reservoir working fluids for egs heat mining. *Geotherm. Resour. Counc. Trans.* **2009**, *33*, 235–239.

9.   Pruess, K. Enhanced geothermal systems (egs) using CO_2 as working fluid—A novel approach for generating renewable energy with simultaneous sequestration of carbon. *Geothermics* **2006**, *35*, 351–367. [CrossRef]

10.   Pruess, K. On production behavior of enhanced geothermal systems with CO_2 as working fluid. *Energy Convers. Manag.* **2008**, *49*, 1446–1454. [CrossRef]

11.   Pruess, K.; Spycher, N. *Enhanced Geothermal Systems (EGS) with CO_2 as Heat Transmission Fluid—A Scheme for Combining Recovery of Renewable Energy with Geologic Storage of CO_2 World Geothermal Congress*; Lawrence Berkeley National Lab. (LBNL): Berkeley, CA, USA, 2010.

12.   Randolph, J.B.; Saar, M.O. Coupling carbon dioxide sequestration with geothermal energy capture in naturally permeable, porous geologic formations: Implications for CO_2 sequestration. In *Proceedings of the 10th International Conference on Greenhouse Gas Control Technologies, Amsterdam, The Netherlands, 19–23 September 2011*; Gale, J., Hendriks, C., Turkenberg, W., Eds.; Elsevier Procedia: Amsterdam, The Netherlands, 2011; Volume 4, pp. 2206–2213.

13.   Randolph, J.B.; Saar, M.O. Combining geothermal energy capture with geologic carbon dioxide sequestration. *Geophys. Res. Lett.* **2011**, *38*. [CrossRef]

14.   Xu, T.; Feng, G.; Shi, Y.; Lei, H. *Use of CO_2 as Heat Transmission Fluid to Extract Geothermal Energy: Advantages and Disadvantages in Comparison with Water*; World Geothermal Congress: Melbourne, Australia, 2015.

15.   Zhang, L.; Feng, L.; Xu, R.; Jiang, P.; Liu, H. Heat transfer and fluid transport of supercritical CO_2 in enhanced geothermal system with local thermal non-equilibrium model. *Energy Procedia* **2014**, *63*, 7644–7650. [CrossRef]

16.   Phuoc, T.X.; Massoudi, M.; Wang, P.; McKoy, M.L. Heat losses associated with the upward flow of air, water, CO_2 in geothermal production wells. *Int. J. Heat Mass Transf.* **2019**, *132*, 249–258. [CrossRef]

17.   Phuoc, T.X.; Massoudi, M.; Wang, P.; McKoy, M.L. Exergy of air, CO_2, and H_2O for use as Geothermal Fluids. *Int. J. Heat Mass Transf.* **2018**, *126*, 448–456. [CrossRef]

18.   Phuoc, T.X.; Massoudi, M. Pumping Gaseous CO_2 into a High-pressure, Constant-Volume Storage Cylinder: A Thermodynamics and Parametric Analysis. *J. Energy Storage* **2021**. submitted for publication.

19.   Phuoc, T.X.; Massoudi, M. On Joule-Thomson cooling capability of compressed CO_2 for energy storage and CO_2 utilization. *J. Energy Storage* **2021**. submitted for publication.

20.   Span, R.; Wagner, W. Equations of state for technical applications. III. Results for polar fluids. *Int. J. Thermophys.* **2003**, *24*, 111–162. [CrossRef]

21.   Vesovic, V.; Wakeham, W.A.; Olchowy, G.A.; Sengers, J.V.; Watson, J.T.R.; Millat, J. The transport-properties of carbon-dioxide. *J. Phys. Chem. Ref. Data* **1990**, *19*, 763–808. [CrossRef]

22.   Fenghour, A.; Wakeham, W.A.; Vesovic, V. The viscosity of carbon dioxide. *J. Phys. Chem. Ref. Data* **1998**, *27*, 31–44. [CrossRef]

23.   NIST. Nist Chemistry Webbook. Available online: http://webbook.Nist.Gov/ (accessed on 30 March 2021).

24.   Kadoya, K.; Matsunaga, N.; Nagashima, A. Viscosity and thermal-conductivity of dry air in the gaseous-phase. *J. Phys. Chem. Ref. Data* **1985**, *14*, 947–970. [CrossRef]

25.   Lemmon, E.W.; Jacobsen, R.T.; Penoncello, S.G.; Friend, D.G. Thermodynamic properties of air and mixtures of nitrogen, argon, and oxygen from 60 to 2000 k at pressures to 2000 MPA. *J. Phys. Chem. Ref. Data* **2000**, *29*, 331–385. [CrossRef]

26.   Lemmon, E.W.; Jacobsen, R.T. Viscosity and thermal conductivity equations for nitrogen, oxygen, argon, and air. *Int. J.* **2004**, *25*, 21–69. [CrossRef]

27.   Kestin, J. *A Course in Thermodynamics*; Revised Printing; McGraw-Hill: New York, NY, USA, 1979; Volume 1.

28.   Wallis, G.B. *One-Dimensional Two-Phase Flow*; McGraw-Hill Publishing: New York, NY, USA, 1969.

29.   Pattanayaka, L.; Padhib, B.N.; Kodamasinghc, B. Thermal performance assessment of steam surface condenser. *Case Stud. Therm. Eng.* **2019**, *14*, 100484. [CrossRef]